REPORT DOCUMENTATION PAGE

Form Approved
OMB No. 0704-0188

1. REPORT DATE *(DD-MM-YYYY)*	**2. REPORT TYPE**	**3. DATES COVERED** *(From - To)*
May 1990	Conference paper	

4. TITLE AND SUBTITLE

See report.

5a. CONTRACT NUMBER

5b. GRANT NUMBER

5c. PROGRAM ELEMENT NUMBER

6. AUTHOR(S)

See report.

5d. PROJECT NUMBER

5e. TASK NUMBER

5f. WORK UNIT NUMBER

7. PERFORMING ORGANIZATION NAME(S) AND ADDRESS(ES)

See report.

8. PERFORMING ORGANIZATION REPORT NUMBER

9. SPONSORING / MONITORING AGENCY NAME(S) AND ADDRESS(ES)

See report.

10. SPONSOR/MONITOR'S ACRONYM(S)

11. SPONSOR/MONITOR'S REPORT NUMBER(S)

12. DISTRIBUTION / AVAILABILITY STATEMENT

Distribution Statement A - Approved for public release; distribution is unlimited.

13. SUPPLEMENTARY NOTES

Presented at the IEEE 1990 National Aerospace and Electronics Conference (NAECON 1990) held in Dayton, Ohio, on 21-25 May 1990.

14. ABSTRACT

See report.

15. SUBJECT TERMS

16. SECURITY CLASSIFICATION OF:			**17. LIMITATION OF ABSTRACT**	**18. NUMBER OF PAGES**	**19a. NAME OF RESPONSIBLE PERSON**
a. REPORT	**b. ABSTRACT**	**c. THIS PAGE**	UU		**19b. TELEPHONE NUMBER** *(include area code)*
Unclassified	Unclassified	Unclassified			

ROBOTIC AIRCRAFT REFUELING: A CONCEPT DEMONSTRATION

M. B. Leahy Jr. V. W. Milholen R. Shipman
Air Force Institute of Technology
Department of Electrical and Computer Engineering
WPAFB OH 45433

ABSTRACT

Application of robotic technologies to aircraft servicing is a research initiative at the Air Force Institute of Technology. Current efforts are concentrated on demonstrating a concept for semi-autonomous ground based robotic refueling. Initially we are assuming that the aircraft's aerial refueling port is within the range space of the refueling manipulator. Navigation issues, while important, are not under investigation. We envision a shared system where a human positions the refueling arm in the vicinity of the aircraft and then allows the refueling port detection and nozzle insertion to be done automatically by a combination of visual servoing and compliant control. A testbed has been developed to support experimental evaluation of the enabling technologies necessary for autonomous refueling. Initial evaluations have successfully demonstrated algorithms for port detection, visual servoing, and compliant control of nozzle motion and insertion. Semi-autonomous robotic refueling is now feasible.

1 Introduction

Within the Air Force, the design and implementation of autonomous robotic systems capable of performing complex tasks will be a major initiative in the coming decade [1]. Because the Air Force may have occasion to perform combat operations in environments contaminated by nerve agents or similar hazards and with fewer skilled personnel available, robotic aircraft turnaround has been studied [4,3]. One complex turnaround task that has been focused on over the past several years is autonomous ground-based aircraft refueling. Ground-based refueling currently requires several military members to accomplish the task, and in a hostile environment, refueling can be cumbersome and difficult [19]. Automated or robotic assisted turnaround will allow operators or supervisors to remain in relative safety while accomplishing mission objectives efficiently. This scenario has several advantages, such as lower personnel requirements, successful operations in normally impossible conditions, and less fatigue and danger for personnel. While the technology exists to field a crude teleoperated refueling system, the enabling technologies for semi-autonomous or fully autonomous operation are not mature.

Initial research in the area of autonomous ground-based refueling was conducted by the Flight Dynamics Laboratory at Wright-Patterson AFB. Their research determined that the air refueling port is the optimal place to refuel aircraft when utilizing a robotic refueling system. This decision was based on accessibility of the port and minimal procedural requirements (i.e., no removal of fuel caps, ease of connecting fuel hoses) for refueling at this location [19]. Figure 1 provides an illustration of this proposed robotic ground-based refueling scheme. A fuel truck is driven into the close vicinity of the aircraft and a robotic refueling boom is placed over the aircraft. The operation of the robotic refueling manipulator in the vicinity of the target aircraft could be automated or left under manual control to locate the refueling port, position, and then insert the refueling nozzle into the port.

A robotics research initiative at the Air Force Institute of Technology (AFIT) is the evaluation of the enabling technologies required for autonomous operation of the port location and nozzle insertion portions of the robotic refueling task. Our approach advocates an intuitive integration of both vision and control technologies. The basic premise is to let each technology do what it does well. Vision systems are good at providing coarse position information. Compliant control schemes utilize force information to compensate for errors in goal position. Proper combination will produce a simple autonomous system for mating the refueling arm and aircraft port.

In our scenario, visual information regarding identification and location of the refueling port is fed back to the robot controller which develops trajectory information needed for robot motion. The autonomous refueling boom will use visual information to close the loop around the motion control problem forming a visual servoing system. The role of the visual servoing system is to place the manipulator (boom) in contact, or close proximity, with the refueling port slipway [20]. An impedance control scheme [4,18] provides the necessary compliance for smooth motion along the refueling port slipway and finally, insertion. Exact knowledge of port location is not required. The inevitable misalignment between robotic refueler and port, caused by errors in calibration and kinematic transformations, is inherently accounted for. The issue of misalignment compensation cannot be overlooked. A conventional robot controller is designed to eliminate all position error by increasing the output torque. Increasing the output torque when the robot is jammed leads to instability and potential damage to the contact surface and/or the manipulator drive system. For a robotic refueling application the slipway is already hardened so the primary concern is additional wear of the manipulator leading to decreased reliability.

The goal of the refueling research project during the last year was to demonstrate the component technologies for our robotic refueling concept. The project was divided into two areas; visual servoing and compliant control. The remainder of this paper describes the research accomplishments that lead to a successful concept demonstration. Section two describes the refueling testbed. Visual servoing research is the subject of section three while implementation and analysis of compliant control of the nozzle is presented in section four. Future research directions are discussed in section five. Conclusions are presented in section six. A more detailed description of our results are in [18,20].

2 Refueling Testbed

Experimental evaluation of theoretical concepts is a vital component of robotics research. The Air Force Institute of Technology Robotic Systems Laboratory has the facilities to demonstrate and evaluate robotic technology for Air Force applications. A block diagram of the laboratory systems used to support robotic refueling research is shown in Figure 2.

2.1 Manipulator

The key component of the refueling mock-up is the PUMA-560 robotic manipulator that simulates the refueling arm. The PUMA-560 is a vertically articulated six degree of freedom (DOF) industrial robot. The six degrees of freedom are three heavy links in a serial configuration and three lighter links in a roll-bend-roll wrist. While the PUMA design is not suggested for eventual implementations it does provide a rigorous test case for the required technologies. Our PUMA has a highly modified control system called ARCADE [16]. The LSI-11/73 processor in the PUMA chassis now serves as a data concentrator, sending joint angles and receiving joint torques, for programs executing on a VAXstation III (ROBBIE). ARCADE supports the experimental evaluation of advanced control algorithms, like impedance control, or allows the user to concentrate on non-control issues, like port recognition, by utilizing the control primitives originally supplied with the VAL-II control system.

2.2 Vision system

The recognition portion of this project is accomplished through the use of a video camera and image processing board. A Sony CCD video camera, Model XC-38, provides the basis for image acquisition, and was attached to the third link of the PUMA-560. The camera's small size and low weight allows for easy usage and minimal impact to manipulator dynamics. An ITEX 100 Image Processing System provides real-time image acquisition and processing of a digitized image. Each image acquired consists of a pixel array size of 512 X 480 12-bit elements. The ITEX board is housed in a VAXstation III (CYCLOP) which provides the computational power for the visual servoing algorithms. By acquiring images and analyzing their content, recognition and position information regarding the refueling port are derived.

2.3 Refueling Apparatus

The simulated refueling port is a half scale mockup of a standard Universal Aerial Refueling Receptacle Slipway Installation (UARRSI). A simple cylinder mounted at the end of a rod connected to the force sensor attached to the sixth link flange simulates the refueling nozzle. These two pieces of refueling hardware were designed by Capt David Duvall from the original UARRSI specifications and produced in the AFIT model shop [4].

2.4 Force Sensor

The PUMA wrist is fitted with a six axis (3 forces, 3 moments) force sensor to provide force feedback. The force sensor subsystem, produced by JR^3, Inc., represents the state of the art and includes the sensor, a local power supply, and processor electronics [12]. The interconnection between the force sensor subsystem and our modified control system (ARCADE) is shown in Figure 3. The sensor subsystem functions independently via its own operating system. Sensor commands are given through the serial port on the electronics package. Force/moment sample rates are user selectable in 1 ms increments. Obtaining the force/moment vector requires; collecting the raw data, transformation to world coordinates, and correct scaling of the sensed forces and moments.

ARCADE uses a parallel interface (DRV11) between the sensor electronics and the data concentrator (11/73) to collect the raw sensor data. Data is scaled to provide fullscale force readings of 111.2 newtons for F_x and F_y and 222.4 newtons for the F_z direction. Interface moments M_x, M_y, M_z are limited to 8.473 newton-meters. Scaled data is sent to ROBBIE where the sensed forces and moments from the tool tip are transformed into world coordinates. The transformation process, developed by Duvall [4], includes correction for gravity based on manipulator position and the masses of the test fixtures.

Force sensor resolution tests indicated that reposition inaccuracies caused repeatability errors for force measurements. The low repeatability mandates conservative resolution limits of ± 6.0 N for forces and ± 2.0 N-m for moments [4] and the use of a deadband limiting function. Additional details about force sensor operations and calibration is contained in [18].

3 Visual Servoing

Our refueling concept requires that the system autonomously locate the aerial refueling port and position the nozzle on the slipway. The desire to refuel without irradiating the aircraft with lasers or ultrasonics, or extensive modifications to existing aircraft systems, lead to an investigation of visual techniques. For autonomous motion to the port the system utilizes the visual information and robot kinematics to provide the desired trajectory and actual location to the robot control system. Closing the control loop around visual inputs is commonly referred to as visual servoing. The area of visual robotic servoing has been receiving greater attention as increased processing power removes some of the past limitations and the demand for fixtureless applications grows. Previous visual servoing research [6,8,5] provided insights but no direct solutions to our unique problems.

The objective of the vision portion of the refueling demonstration was for the refueler (PUMA-560) to visually scan for the refueling port, and upon identification, provide the correct joint positions (based on port cartesian coordinates) necessary to servo the end-effector (refueling nozzle) onto a stationary slipway. A thorough investigation of port recognition techniques was beyond the scope of this initial research effort. Our recognition objective was to implement a simple algorithm that could demonstrate the visual servoing concept and serve as a baseline for future research. The Robotic Visual Servoing System (RVSS) has been developed to meet those objectives and was able to successfully demonstrate the concept of visual servoing for robotic refueling.

3.1 Receptable Recognition

The refueling aircraft is a cooperative target to the refueling system. Therefore passive indicators should be employed to reduce the complexity of the recognition task. The indicators chosen for this research were three white rectangular strips. White was chosen so that these indicators were the whitest objects in the area of the refueling port (compared to the gray primer background). White was not a requirement; its use merely simplified the recognition algorithm. A different color choice just requires resetting the threshold levels in the histogram algorithm. Two of the indicators where placed along the side of the slipway while the other was placed along the top, as shown in Figure 4. The indicators formed a three sided box around the refueling port, thereby allowing the center of the box to be roughly the desired port position of contact. Three indicators were deemed the minimal number required to provide center of mass, pose and pattern uniqueness data.

The location of the port was not know a priori and the camera had a limited field of view. Therefore a necessary component of the recognition processes was the ability to search the robot's range space. A search pattern was developed that servoed the PUMA-560 through a predetermined point-to-point search path [20]. At each point, an image was acquired of the environment and passed to the recognition algorithms for processing. In the event that the port was determined not to be in the current image, the search would continue by servoing the PUMA-560 to the next search point and again an image would be acquired and analyzed.

After an image was acquired, a histogram was performed on the image and the subsequent data stored in an array. Starting at the white end of the spectrum (pixel value 255) and regressing, an element of the histogram array was compared to its two neighbors to detect a peak. In short, was the element in question larger than its two neighbors? If the number of pixels with this peak value or greater

was larger than 25, then this pixel value was considered the white pixel value. The value 25 was chosen to eliminate the possibility of small peak detection; peaks too small to be the desired peak value. In order to provide flexibility about this value, the white pixel value was decreased by 10 percent of its value; thereby, providing a new pixel value considered to be the white limit. Any pixel whose value was equal to or greater than the white limit was considered white, everything else was considered black, and the image thresholded appropriately.

Through extensive analysis of images containing the three indicators but with the port's distance from the PUMA varied, a range area of the number of white pixels capable of representing the three indicators was determined. If the number of white pixels in the image was less than 100 or greater than 100,000, then the refueling port was considered not to be in the image and no further recognition processing would be conducted on this image. If the number of white pixels was within this range, then the center of mass of these white pixels was found. By manipulating the Y center of mass coordinate, the image was divided in half. The top half would naturally contain the top indicator, and the bottom half contained the two bottom indicators. In addition the bottom half of the image was further divided in half to separate the two bottom objects. By scanning from top to bottom and left to right in each of these areas, the top, bottom, left and right sides (row and column locations) were derived.

When objects had been located in each of the three areas, simple geometric logic was used to ensure that the objects found were truly the three indicators. These tests included height-to-width and width-to-height ratios, as well as locations of object sides to the sides of the other objects. Upon satisfying all the logic requirements, the port was considered identified.

3.2 Servoing

Based on the width of the top indicator, the range of the port to the camera was derived [20]. With that value, the range from the base of the PUMA was derived and its cartesian location found based on the forward kinematics equations developed for the first three links of the PUMA by Fu, Gonzalez and Lee [7]. With the location and range parameters of the port known, the inverse kinematics were derived through simple Law of Cosines equations. The desired joint position of the port was transmitted to the LSI-11/73 which executed a simple program based on VAL-II primitives to servo the arm to that location. The RVSS could place the nozzle within 10 cm of the refueling port. That level of accuracy provides an acceptable starting point for a compliant insertion algorithm.

4 Compliant Control

The primary objective of this portion of the refueling project was to accomplish a simulated refueling port connection between a refueling nozzle and the UARRSI port using the PUMA-560 robot under active compliance control. While visual servoing is a necessary part of an autonomous refueling system, it is inappropriate for fine motion task control. A simple analogy is putting a record on a spindle. You need your vision system to provide an approximate location of the hole relative to the spindle, but the actual insertion is usually accomplished by *feel* once the record and shaft are in contact. Compliant control provides a robot with the ability to mimic a human's ability to *feel* i.e. comply with the environment.

The requirement to comply with the environment, and not necessarily command contact forces, was the basis for our selection of an impedance control approach. Several forms of impedance control have been evaluated on experimental robots [11,13] and end-effectors [14]. The demonstrated potential of the approach lead to an effort to evaluate impedance control for robotic refueling applications. Implementation on our PUMA was started in 1988 by Capt David Duvall [4]. Subsequent research provided the refinements necessary to successfully demonstrate the advantages of compliant refueling [18].

A basic premise of the impedance control method is that once in contact with the environment the manipulator should assume the characteristics of an impedance [9,11]. Therefore the task of the controller is to regulate the robot's output impedance, not its motion. A commonly assumed target impedance, referred to as the desired dynamics by Hogan [9], is expressed as:

$$F_{int} = K(x_0 - x) + B(v_0 - v) + M\frac{dv}{dt} \tag{1}$$

The damping(B), stiffness(K), and inertia(I) of the environment (an admittance) determine the most effective manipulator impedance to maintain during trajectory tracking.

4.1 Implementation

The form of nonlinear impedance control implemented in this study [18] was first derived by Hogan [10] and modified for the refueling problem by Duvall [4].

$$\begin{aligned}\tau_{act} = \; & I(q)J^{-1}M^{-1}K[x_0 - L(q)] + S(q) \\ & + I(q)J^{-1}M^{-1}B[v_0 - J\dot{q}] + V(\dot{q}) \\ & - [J^T + I(q)J^{-1}M^{-1}]F_{int}\end{aligned} \tag{2}$$

where:

q is the measured joint position

$\dot{q}$ is the computed joint velocities

I is the manipulator inertia matrix

J^{-1} is the inverse Jacobian matrix

M^{-1} is the inverse desired mass matrix

K is the desired stiffness matrix

x_0 is the commanded position

L is the position from forward kinematics

S is the gravity compensation term

B is the desired damping matrix

v_0 is the commanded velocity

V is the friction compensation

J^T is the Jacobian transpose

F_{int} is the interface force between constraint and manipulator

Feedforward compensation ($S(q), V(\dot{q})$) is used to linearize the nonlinear dynamics while multiplication by the inertial matrix ($I(q)$) decouples the dynamics and accounts for variations in robot inertia. The inverse Jacobian and inverse kinematics solve the coordinate space problem.

While an impedance control law can be written for a full 6 DOF robot we restricted our initial research to 2 DOF. The shoulder and elbow joints of the PUMA provided a rigorous test of the impedance concept without the computational complexity required for higher order implementation. The forward kinematics, Jacobian, and inverse Jacobian are all calculated from symbolic equations derived by MACSYMA [18]. Inertial parameters, dynamics equations, and friction compensation are identical to those employed in previous gross motion control studies [17,16]. The M, K, and B terms are all diagonal matrices and are input as control parameters for each unique application. Use of a diagonal mass matrix reduces M^{-1} to simple division. Our values for M, B, and K were selected by trial and error with a sequence of gains used to determine a set of values that would indeed minimize interface force and still maintain contact [18]. The impedance coefficients ($IJ^{-1}M^{-1}$), ($IJ^{-1}M^{-1}B$),

$(IJ^{-1}M^{-1}K)$, $(IJ^{-1}M^{-1}BJ)$, and $(J^T + IJ^{-1}M^{-1})$ were computed offline and stored for each sample point. A balance between maximum control law sample rate and acceptable force sensor reliability was found at 5.4 ms for our implementation.

4.2 Test Conditions

A robotic manipulator which carries the refueling nozzle must:

- move to the slipway,
- maintain surface contact,
- apply minimal force to the surface,
- overcome jamming at the port, and
- enter the refueling port.

To evaluate the impedance controller's ability to meet those requirements the robot was commanded to track a simple trajectory. The test trajectory, shown in Figure 5, consists of two segments, a vertical drop and a forward sweep. This trajectory was designed to drop onto the refueling port slipway with commanded position going *below* the slipway surface and then moving forward into the refueling port. This motion provided continuous contact with the environment in the constrained case. The trajectory was tailored to have the correct orientation since two degrees of freedom will not overcome misalignments that are out of the xz plane.

4.3 Results and Analysis

Prior to refueling concept demonstration the impedance control law went through a series of tests designed to validate algorithm performance [18]. An unconstrained refueling test, i.e. the test trajectory without port contact, reaffirmed the freespace trajectory tracking capabilities of the impedance control law, demonstrated stability and proper force sensor operation. The ability to successfully follow the constrained refueling trajectory demonstrated the feasibility of our concept for autonomous nozzle insertion through impedance control.

Position errors from the nozzle insertion demonstration are plotted in Figure 6. Several important points in the trajectory are easily seen from these plots. Three points in time will be identified for reference. At approximately 10 seconds, the probe first contacts the slipway. Once contact begins, it is never lost. At the 15 second point (half way through the trajectory), the trajectory changes from vertical motion to horizontal motion. At approximately 28 seconds, the refueling probe steps over the entry lip and enters the refueling port. These three transitions are quite distinctive in the plots of cartesian position errors and interface forces. Once contact is made the position errors begin to build up rapidly. Commanded motion is in the vertical direction only until the 15 second point so the expected error is only in the z direction. However, the actual error is shared almost equally between the x and z directions. The interface force is all in the z direction as expected. The control law splits this input into two torques based on the impedance coefficients. These torques counteract the continually increasing position torque (Figure 7) developed from the position error. The resultant command torque seen in Figure 8 exhibits a characteristic that is relatively flat over the entire test. This active compliance capability is the reason impedance control is ideal for application to the refueling task. The robot remains stable and the contact force is minimized.

As the nozzle moved down the slipway incline, position errors decreased and interface forces lessened. This trend continued until the nozzle encountered the metal housing around the port. The lip at the bottom of the slipway was an obstacle that was detected and compensated for. Instead of jamming, the nozzle slipped into the port. Obviously, motion was much more restricted once a connection was completed, and data plots show more damped operation once the nozzle is connected to the port. It is important to note that trajectory tracking was never lost even when position error was greatest. This test was very repeatable, but terminal position was also somewhat dependent on the calibration point. Even under benign laboratory conditions perfect knowledge of port position is not feasible.

5 Discussion

While our evaluations clearly demonstrated the feasibility of our refueling concept they also highlighted several limitations. The port recognition algorithm was not very robust to changes in lighting conditions. Early in the project priority was given to developing the support structure for visual servoing and not to port recognition development. The existing computational environment was also insufficient to support the complex algorithms necessary for brightness invariance. However the computational environment has been upgraded with the addition of an AP30 Vaccelerator [2] and efforts to implement a robust port recognition algorithm based on the brightness invariance techniques developed by Lambert [15] are underway. A dynamic visual servoing algorithm is also under development to remove the stationary port restriction.

To demonstrate a more realistic scenario of the actual nozzle insertion procedure the degrees of freedom under impedance control must be increased. Once the control law is extended to the base joint of the PUMA we will be able to remove the fixturing requirements of the initial demonstration and autonomously insert the nozzle from any location in the refueler workspace. With the force sensor subsystem now fully integrated into ARCADE the investigation of alternative compliant control techniques is underway. Knowledge of the tradeoffs between employment of passive or active compliant control schemes will provide valuable information for actual system design.

6 Conclusion

Robotic aircraft refueling systems will inhabit the flightline of the future. A refueling testbed has been developed at the Air Force Institute of Technology Robotic Systems Laboratory to support development and evaluation of the enabling technologies that will make robotic refueling a reality. Initial research has concentrated on automating the refueling task once the aircraft is within the refueler's range space. We have successfully demonstrated a concept for autonomous nozzle insertion that utilizes techniques of visual servoing and impedance control. Current research is concentrated on improving the robustness of the port recognition algorithm and increasing the number of degrees of freedom under impedance control. Further research will provide the refinements necessary for full scale development.

7 Acknowledgments

This research was partially sponsored by the Wright Research and Development Center.

References

[1] Air Force Studies Board, *Advanced Robotics for Air Force Operations*, National Academy Press, Washington, D. C. 1989.

[2] Avalon Computer Systems, Inc. "Vaccelerator Operation's Manual." Glendale, California: June 1989.

[3] Battelle Corp., *Concept Development for Robotic Aircraft Turnaround: Final Task II Report*, Columbus OH: Battelle Columbus Laboratories, 1989.

[4] Duvall, D.J. *Robotic Compliant Motion Control for Aircraft Refueling Applications*. AFIT/GA/ENG/88D-1 Air Force Institute of Technology, Air University, December 1988.

[5] Feddema, J. T. and O. R. Mitchell. "Vision-Guided Servoing with Feature-Based Trajectory Generation." *IEEE Trans. on Robotics and Auto.*,Vol 5, pp. 691-700, October 1989.

[6] Gershon, David and Isaac Porat. "Vision Servo Control of a Robotic Sewing Machine," *Proc. of the IEEE Int. Conf. on Robotics and Auto.*, pp. 1830-34, 1988.

[7] Fu,King-Sun,R.C. Gonzalez, and C.S.G. Lee. *Robotics: Control, Sensing, Vision, and Intelligence.* New York: McGraw-Hill Book Company, 1987.

[8] Harrell, R. C. and others. "Vision Guidance of a Robotic Tree Fruit Harvester," *Intelligent Robots and Computer Vision,* Vol 579, pp. 537-45, 1985.

[9] Hogan, N. "Impedance Control: An Approach to Manipulation, Part I - Theory," *ASME J. of Dyn. Sys., Meas. and Control,* Vol 107, pp. 1-7, March 1985.

[10] Hogan, N. "Impedance Control: An Approach to Manipulation, Part II - Implementation," *ASME J. of Dyn. Sys., Meas. and Control,* Vol 107 pp. 8-16, March 1985.

[11] Hogan, N., "Stable Execution of Contact Tasks Using Impedance Control," *Proc. of the IEEE Int. Conf. on Robotics and Auto.*, pp.1047-1054, 1987.

[12] JR3 Inc. *Universal Force-Moment Sensor System Operation Manual.* JR3,Inc, Woodland,CA, July 1988.

[13] Kazeronni, H., "Automated Deburring Using Electronic Compliancy: Impedance Control", *Proc. of the IEEE Int. Conf. on Robotics and Auto.* , pp.1025-1032, 1987.

[14] Kazeronni, H., "Direct-Drive Active Compliant End-effector", *IEEE J. af Robotics and Auto.*, Vol. 4, No. 3, pp. 324-333, June 1988.

[15] Lambert, Capt. Lawrence C. *Evaluatian and Enhancement af the AFIT Autonomous Face Rcognition Machine.* MS Thesis, AFIT/GE/ENG/87D-35. School of Engineering, Air Force Institute of Technology (AU), Wright-Patterson AFB, OH, December 1987.

[16] Leahy, M.B. Jr. "Experimental Analysis of Robot Control: A Performance Standard for the PUMA-560", *Proc, of the IEEE 4th Int. Symp. on Intel. Control*, pp. 257-64, Sep 1989.

[17] Leahy, M.B. Jr. and G.N.Saridis, "Compensation of Industrial Manipulator Dynamics" *The Int. J. af Robotics Research*,Vol 8, No, 4, pp. 73-84,August 1989.

[18] Milholen, V.W., *Experimental Evaluation of Impedance Control for Robotic Aircraft Refueling* MS Thesis, AFIT/GE/ENG/89D-32. School of Engineering, Air Force Institute of Technology (AU), Wright-Patterson AFB, OH, December 1989.

[19] Miller, Capt. Mikel M. *Implementation of a Visual Servoing System for Evaluation of Robotic Refueling Applications.* MS Thesis, AFIT/GE/ENG/87D-45. School of Engineering, Air Force Institute of Technology (AU), Wright-Patterson AFB, OH, December 1987.

[20] Shipman, R. P., *Visual Servoing for Autonomous Aircraft Refueling.* AFIT/GE/ENG/89D-48 Air Force Institute of Technology, Air University, December 1989.

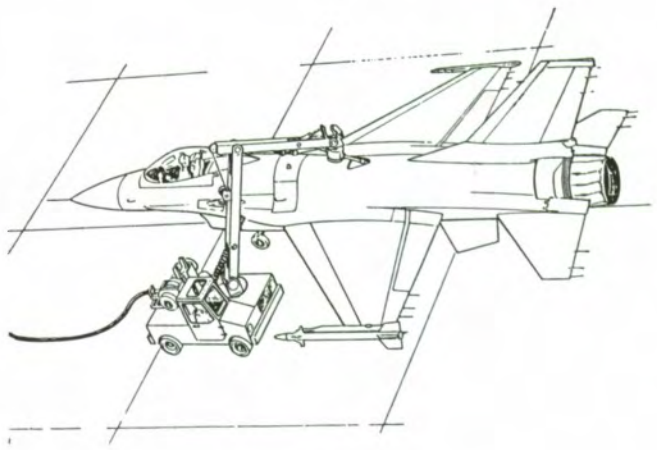

Figure 1: Robotic Refueling Concept

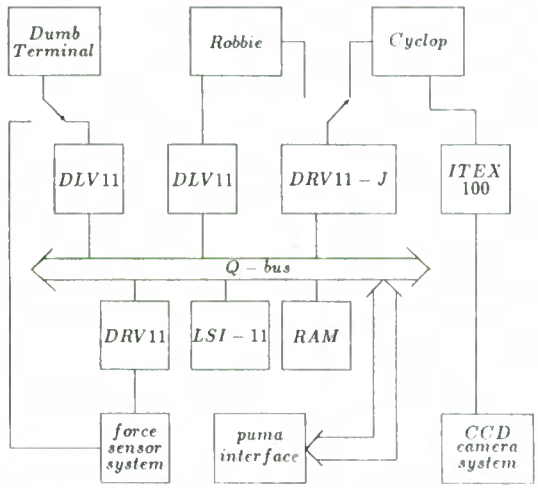

Figure 2: Robotic Refueling Project Laboratory Support System Diagram

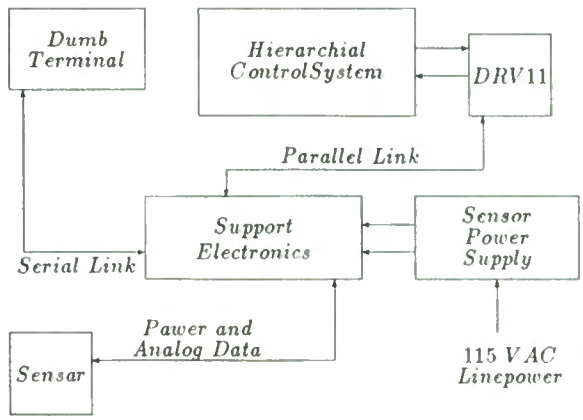

Figure 3: Force Sensor Subsystem Block Diagram

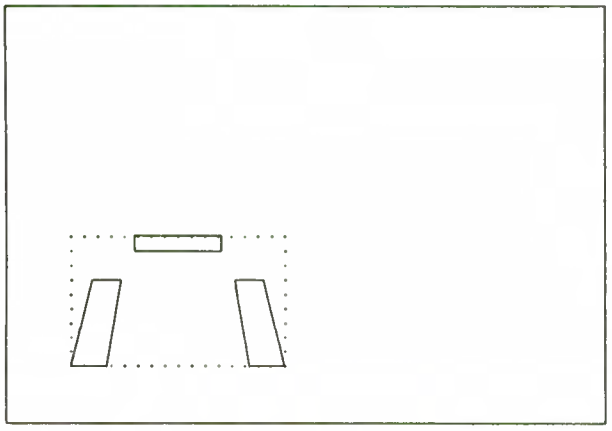

Figure 4: Placement of Indicators

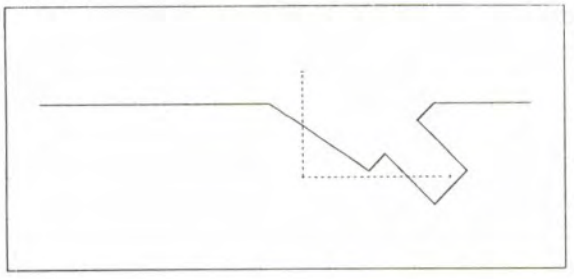

Figure 5: Refueling trajectory from positive Y viewpoint into the XZ plane. Note the track is *beneath* the refueling port.

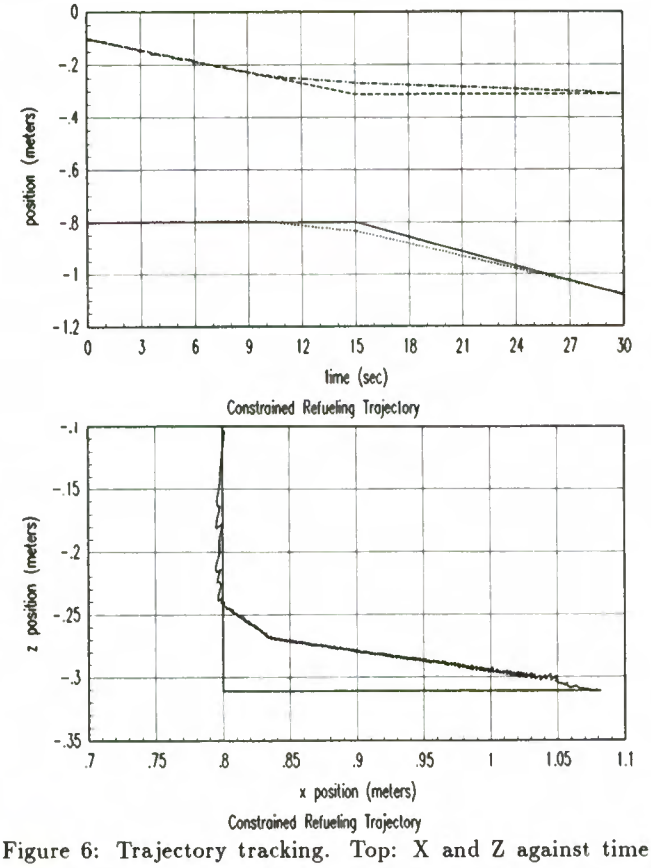

Figure 6: Trajectory tracking. Top: X and Z against time. Dotted traces are actual trajectories, X on lower half of plot, Z on upper. Bottom: X and Z in a spatial representation of the workspace.

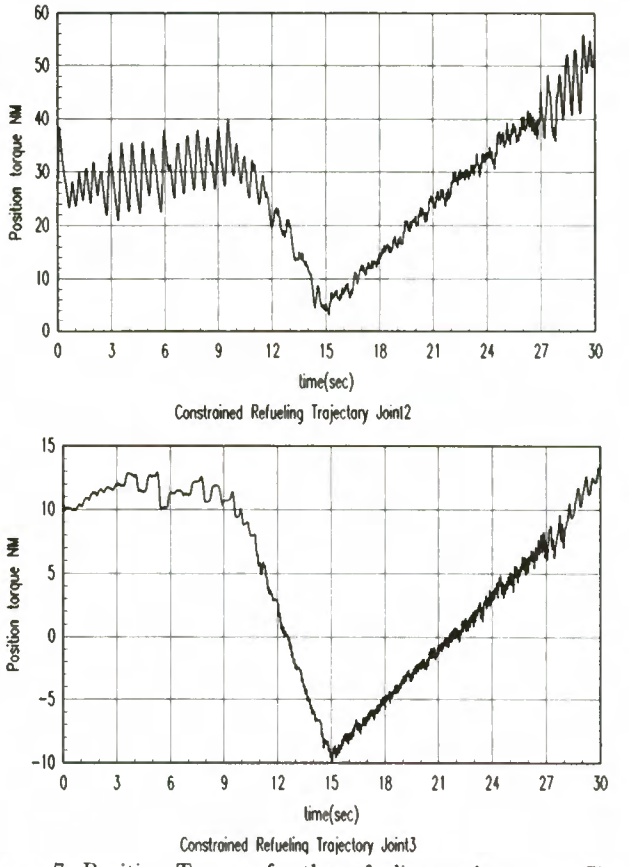

Figure 7: Position Torques for the refueling trajectory. Top: joint 2 Bottom: joint 3

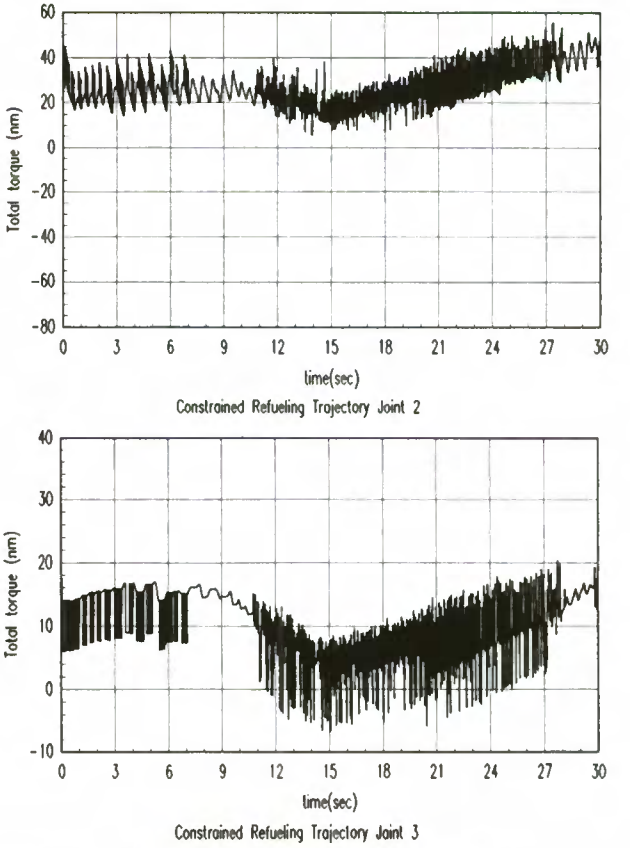

Figure 8: Total Torques for the refueling trajectory. Top: joint 2 Bottom: joint 3